Nano Energy 86 (2021) 106121

Contents lists available at ScienceDirect

Nano Energy

journal homepage: www.elsevier.com/locate/nanoen

Full paper

Highly flexible radial tandem junction thin film solar cells with excellent power-to-weight ratio

Shaobo Zhang [a], Ting Zhang [a], Zongguang Liu [a], Junzhuan Wang [a,*], Linwei Yu [a,*], Jun Xu [a], Kunji Chen [a], Pere Roca i Cabarrocas [b]

[a] National Laboratory of Solid State Microstructures/School of Electronics Science and Engineering/Collaborative Innovation Center of Advanced Microstructures, Nanjing University, 210093 Nanjing, PR China
[b] LPICM, CNRS, Ecole Polytechnique, Institut Polytechnique de Paris, 91128 Palaiseau, France

ARTICLE INFO

Keywords:
Radial tandem junction solar cells
Flexible thin film
Power-to-weight ratio

ABSTRACT

High power-to-weight ratio (PTWR) is an important figure-of-merit for high performance flexible/portable solar cells. Marrying advanced tandem junction design with three-dimensional (3D) Si nanowire (SiNW) framework enables a promising route to boost the PTWR. In this work, a radial tandem junction (RTJ) thin film solar cell has been demonstrated, for the first time, over SiNWs, which consist of radially deposited *p-i-n* multilayers with hydrogenated amorphous silicon (a-Si:H) and hydrogenated amorphous silicon germanium (a-SiGe:H) absorption layers in the outer and the inner junctions, respectively. The strong light trapping within the 3D SiNW framework allows for the use of a very thin a-SiGe:H (~45 nm) absorption layer to harvest efficiently the long wavelengths. The RTJ cells fabricated via a one-pump-down process in a single PECVD chamber, directly upon 15 μm thick aluminum foils demonstrate an excellent flexibility that can bend to 10 mm radius and achieve a record PTWR~1628 W/kg, and accomplish a high open-circuit voltage, filling factor and conversion efficiency of 1.2 V, 61.5% and 8.1% on glass, respectively, substantially improved compared to those accomplished by radial single junction cells. These results highlight the unique potential of 3D radial tandem technology to enable a new generation of high performance and durable flexible photovoltaics.

1. Introduction

Hydrogenated amorphous silicon (a-Si:H) thin film solar cells are an industrially-proven photovoltaic technology [1–5] that has been the ideal choice for building a plethora of flexible/portable, light-weight and durable photovoltaics [5–7] and biomimetic/bio-friendly photodetectors [8,9]. In order to boost the conversion efficiency further and adapt to the emerging needs of highly flexible and high power-to-weight ratio (PTWR) photovoltaics, more advanced tandem solar cell structures have to be used to broaden the light absorption spectrum, which is limited to $\lambda < 700$ nm for the a-Si:H thin-film due to its wider optical bandgap of 1.75 eV. The tandem solar cells adopt two *p-i-n* junctions with wider/narrower bandgaps in the front/rear absorption layers to harness a wider solar spectrum and deliver a higher photo-voltage output, for example, the commercially available planar tandem a-Si:H/microcrystalline silicon (μc-Si:H, with a bandgap of ~1.1 eV) solar cells [10–16]. However, these Si thin film tandem solar cells, with a thick bottom μc-Si:H layer (~2 μm in order to capture the long wavelengths) are not very flexible, and the long deposition duration >2 h at a rate of ~0.3 nm/s [11,13,15,17] by using plasma-enhanced chemical vapor deposition (PECVD), is a huge burden for further cost reduction, as well as a fundamental limitation for developing high PTWR performance tandem solar cells.

Actually, the need of such a thick bottom layer of μc-Si:H can be exempted within a 3D radial junction framework, built over standing Si nanowires (SiNWs), where the optical absorption path and the electric separation distance are decoupled [18–23], as witnessed in our previous works for radial single junction (RSJ) a-Si:H solar cells [3,5,24–26] constructed over SiNWs grown via vapor-liquid-solid (VLS) mechanism [27–29]. Unfortunately, depositing a conformal layer of high quality μc-Si:H on the sidewall of SiNWs is rather difficult, as the formation of crystalline phase relies heavily on the ion bombardment effect in the plasma [30,31]. An ultimate solution to address this challenge is to adopt another low-bandgap thin film material such as hydrogenated amorphous silicon germanium (a-SiGe:H), which has been used in planar tandem solar cells [2,32–35], with a narrower and tunable

* Corresponding authors.
E-mail addresses: wangjz@nju.edu.cn (J. Wang), yulinwei@nju.edu.cn (L. Yu).

https://doi.org/10.1016/j.nanoen.2021.106121
Received 26 November 2020; Received in revised form 24 March 2021; Accepted 24 April 2021
Available online 4 May 2021

bandgap (by varying the Ge content) that allows a broader external quantum efficiency (EQE) response [36–39], compared to that of a-Si:H solar cells, as seen for example Fig. 1b. However, such a radial tandem junction (RTJ) solar cell structure has never been explored in the literature.

In this work, we demonstrate the first ever radial tandem junction (RTJ) thin film solar cells, consisting of stacked *p-i-n* junctions with a-Si:H (outer) and a-SiGe:H (inner) absorber layers deposited conformally over VLS-grown SiNWs. Based on optimized SiNW structure and a series of critical parameter controls over the Si/Ge content ratio, the layer thicknesses and the tunneling junction designs, RTJ solar cells with ultrathin a-Si:H (~55 nm) and a-SiGe:H (~45 nm) absorber layers have been successfully fabricated upon glass and Al foil substrates, with greatly improved device performance compared to the planar reference and single junction counterparts, as well as excellent flexibility allowing to bend down to a 10 mm radius and a new record PTWR~1628 W/kg. These results represent the highest performance of the flexible Si thin film RTJ solar cells constructed on the VLS-grown SiNWs with a record PTWR value, which are ideal candidates for the construction of a new generation of flexible and durable photovoltaics, catering to the needs of the booming markets in portable and wearable electronics [40–42].

2. Experiments

2.1. Device fabrication

The RTJ solar cells were fabricated upon tin (Sn) catalyzed VLS-growth of SiNWs over Al-doped Zinc Oxide (AZO) coated glass and Al foil (15 μm thick) substrates, with a coaxial multilayer structure of p-type SiNWs/intrinsic a-SiGe:H/n-type a-Si:H/p-type a-Si:H/intrinsic a-Si:H/n-type a-Si:H/ITO, as depicted schematically in Fig. 1a. First, a nominal 4 nm thick Sn layer was evaporated to the surface of AZO glass, which was then treated by a hydrogen (H_2) plasma for 5 min, at a substrate temperature, H_2 flow rate, RF power density and chamber pressure of 200 °C, 20 standard cubic centimeter per minute (SCCM), 10 mW/cm^2 and 30 Pa, to remove the surface oxide layer and transform the Sn layer into discrete droplets, with tunable density and diameters. Then, a mixture of 60 SCCM H_2, 6 SCCM silane (SiH_4) and 1.8 SCCM diborane dopant (B_2H_6) precursor gases was introduced to grow p-type SiNWs at substrate temperature, RF power density and chamber pressure of 350 °C, 20 mW/cm^2 and 100 Pa, respectively, for 15 min (see Fig. 1d). Third, an intrinsic a-SiGe:H alloy layer was deposited around the SiNWs, by a plasma of 20 SCCM H_2, 6 SCCM SiH_4, with some amount of GeH_4 (95% H_2-diluted), at 150 °C, followed by the deposition of n-type a-Si:H layer, with a mixture of 20 SCCM H_2, 6 SCCM SiH_4 and 2.3 SCCM phosphine (PH_3) as precursor gases. Then, the second *p-i-n* junction was deposited by repeating the above-mentioned growth steps, except that now the p-SiNWs and the a-SiGe:H layer were replaced by a

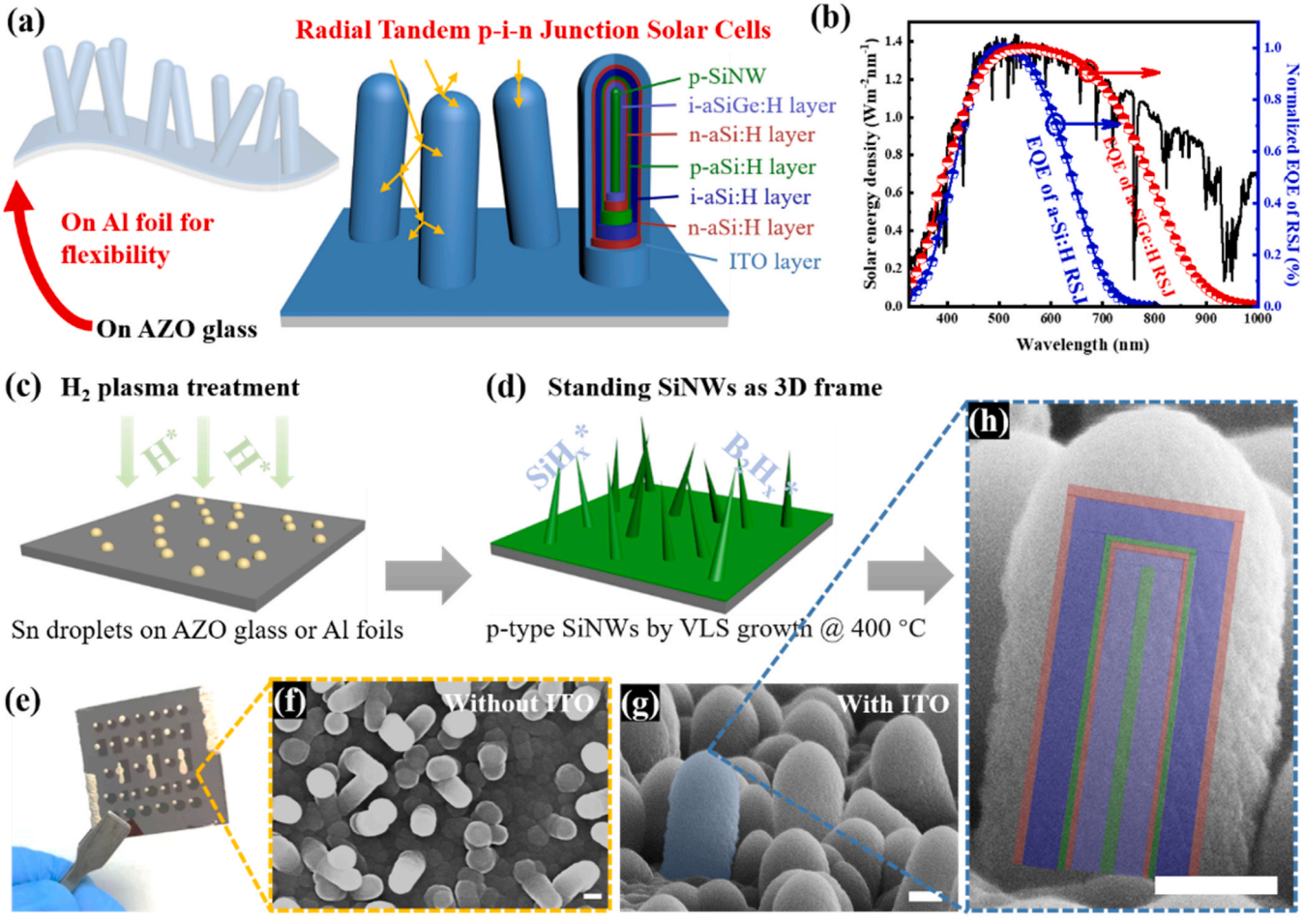

Fig. 1. The complete RTJ configuration (with ITO layer) and flexible RTJ solar cell fabricated on Al foil are depicted in (a). The solar energy spectra, and normalized EQE of radial single junction are plotted in (b). The illustrations of the fabrication procedure on AZO-glass substrate: (c) Sn catalyst formation via H_2 plasma treatment, followed by (d) the VLS growth of p-type SiNWs from a mixture of H_2, SiH_4 and B_2H_6. (e) the picture of RTJ solar cells, where the active areas with ITO appear darker. The SEM images of the as-grown RTJs are shown in (f, top-view without ITO) and (g, h, side-view with ITO), respectively. Scale bar is 200 nm for all.

p-type a-Si:H layer and an intrinsic a-Si:H layer. Finally, ITO top electrode pads were deposited upon the RTJs through a shadow mask by using magnetron sputtering, which allows the incident light to shed in through the top transparent ITO electrodes.

2.2. Device characterizations

The morphology of the RTJ structures was characterized by scanning electron microscopy (SEM, Zeiss Sigma). The photocurrent density-voltage (*J-V*) characteristics were measured under standard AM 1.5 G illumination conditions (Newport, Oriel Sol-1A), while the external quantum efficiency (EQE) response was measured with a calibrated silicon detector by using QE-R system from Enli Tech within a wavelength range from 300 nm to 1000 nm and a sweep step of 10 nm. The light absorption was characterized by using a UV–Vis–NIR Spectrophotometer (UV-3600 Plus, Shimadzu).

3. Results and discussion

Fig. 1e shows a photograph of the RTJ solar cells fabricated on a glass substrate, while SEM images of the RTJ structures deposited over the SiNWs, with or without final ITO coating, are presented in Fig. 1g and f, respectively. An enlarged side view of a selected RTJ unit is displayed in Fig. 1h, which has an inner coaxial multilayer structure as depicted schematically in Fig. 1a. According to the statistics presented in Fig. S1, the standing RTJs have rather uniform diameters, measured at the top or the root segments, and both are around $D_{RTJ} \sim 430$ nm (with ITO layer), with a height of $H_{RTJ} \sim 1000$ nm determined for the longest RTJ units in SEM images. This indicates a quite conformal coating of the multilayer thin films over the 3D SiNW framework, which is a criterion for the construction of high-quality radial junction solar cells. To examine the internal RTJ structure that should have a coaxial multilayer arrangement as indicated in Fig. 2a, selected RTJ units were broken using a nano-manipulator to reveal the cross-sections, as seen for example in the two SEM images shown in the left panels of Fig. 2c and d. Interestingly, the inner and the outer *p-i-n* junction regions show slightly different contrast in the SEM images due to the presence of Ge in the inner cell, and thus allow us to extract and verify the corresponding layer thicknesses. As seen in the statistics shown in the right panels of Fig. 2c and d, the outer a-Si:H and the inner a-SiGe:H absorber layer thicknesses are found to be around $t^{outer}_{a-Si} = 56 \pm 5$ nm and $t^{inner}_{a-SiGe} = 45 \pm 6$ nm, which are extracted from five samples at 149 different sites as shown in Fig. S2, for the sample with deposition durations of 40 min and 30 min, respectively. Both of them are much smaller than the typical layer thicknesses used in planar junction solar cells [33,34,43–45].

The band profile of the RTJ solar cells at equilibrium is schematically drawn in Fig. 2b, where E_c, E_v and E_f are the bottom of conduction band, the top of valence band and the Fermi energy level, respectively. When the light is shed through the outer/top transparent ITO electrodes, photocarriers are generated in both the outer and the inner absorber layers, and then separated by the built-in fields in corresponding PIN junctions. At the middle joint interface, the photo-generated electrons and holes recombine to deliver a photocurrent that runs through the stacked PIN junctions in series. As a key parameter to adjust the absorption bandgap of a-SiGe:H thin film, the GeH_4 flow rate and thus the Ge content in the deposited thin film, was first tuned with a constant SiH_4 flow rate of 6 SCCM. As shown in Fig. 3a, the optical bandgap, extracted by measuring the absorption spectra and Tauc fitting [46,47],

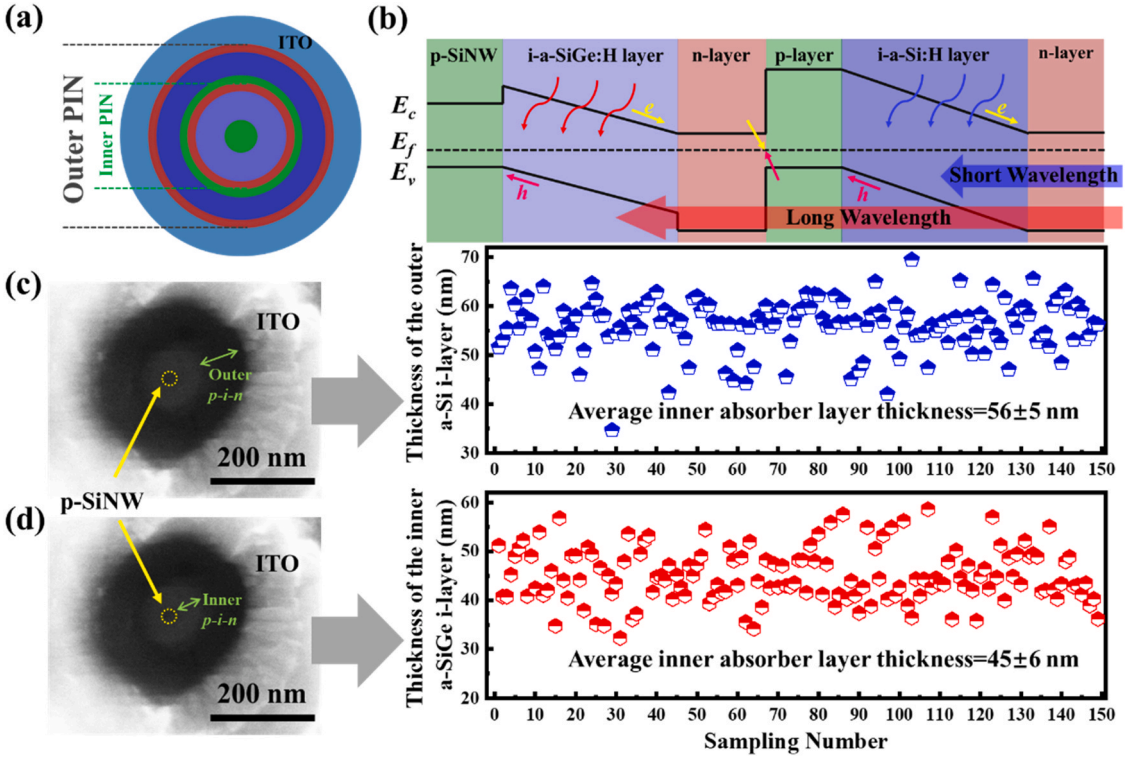

Fig. 2. The diagram of cross section of RTJ is plotted in (a), and the band diagram of RTJ is depicted in (b). The SEM image of cross section of RTJs is shown in the left panels of (c) and (d), respectively, for the statistics of thickness of outer and inner absorber layers are depicted in the right panels.

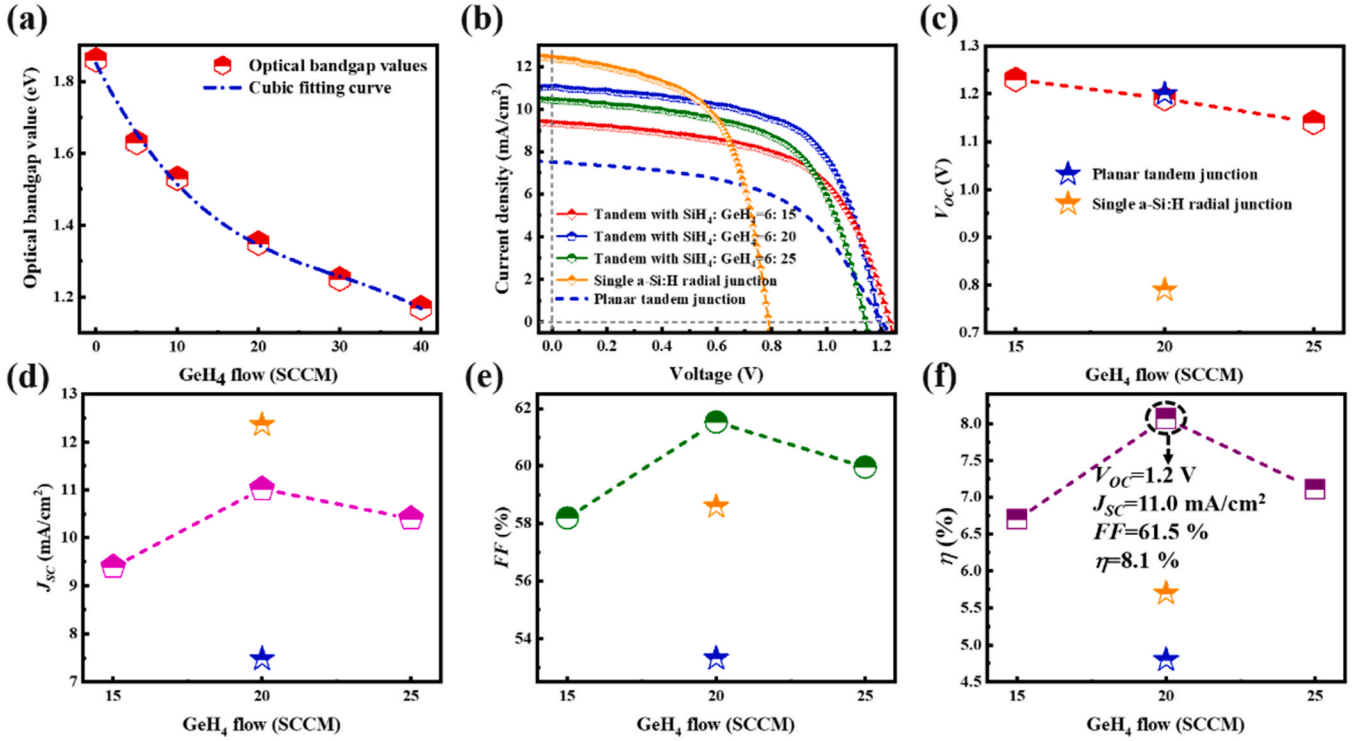

Fig. 3. The E_g value vs GeH_4 flow rate when that of SiH_4 is 6 SCCM is plotted in (a). The (b) *J-V* curves, (c) V_{OC}, (d) J_{SC}, (e) *FF* and (f) η of the fabricated RTJ solar cells on AZO glass vs different GeH_4 flows are shown, respectively, in comparison to the planar tandem junction and radial single junction.

decreases monotonically with the increase of GeH_4 flow rate. By choosing the optimized a-Si:H *p-i-n* junction parameter conditions, a series of RTJ cells were fabricated with varied GeH_4 flow rates, along with reference cells of a-Si:H RSJ and planar tandem junction. The *J-V* curves of the devices were measured under standard AM 1.5 G illumination and shown in Fig. 3b, while the key performance parameters of open-circuit voltage (V_{OC}), short-circuit current (J_{SC}), fill factor (*FF*), power conversion efficiency (η) are displayed in Fig. 3c–f, respectively.

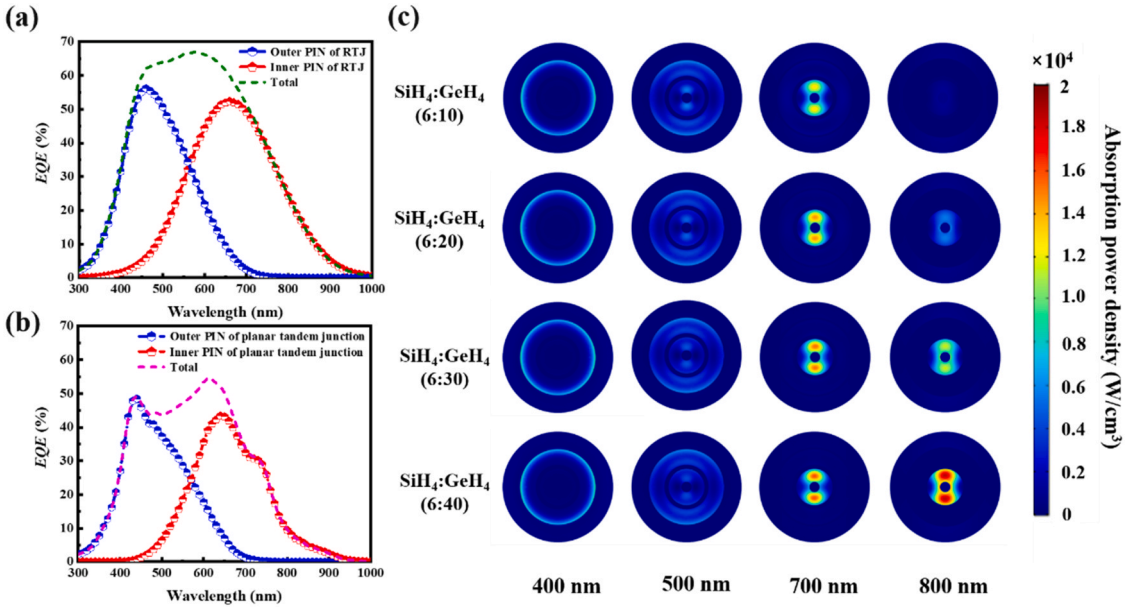

Fig. 4. Experimental EQE curves of RTJs and planar tandem junctions are depicted in (a) and (b), respectively, where the inner absorber layers are fabricated with flow ratio of SiH_4:GeH_4 being 6:20. The simulated light absorption patterns extracted from the cross-section surfaces at the half height of the RTJ cells for different incident wavelengths and with different Ge contents are presented in (c).

It is found that, while the V_{OC} always decreases slowly with the increase of Ge content (as expected), all other parameters demonstrate a similar trend that peaks at the GeH_4 flow rate of 20 SCCM. The first stage of J_{SC} increase can be assigned to the increased light absorption when the optical bandgap is reduced with higher Ge content, while the drop of J_{SC} and *FF* at even higher Ge flow rate/content could result from the increased defect density in the high Ge-content a-SiGe:H thin films that can lead to a faster photocarrier recombination [48–50]. Therefore, in the following experiment, the GeH_4 flow rate of 20 SCCM was chosen and fixed for the deposition of the inner a-SiGe:H layer, which according to Fig. 3a should produce an absorption bandgap of $E_g \sim 1.35$ eV. The impact of the inner a-SiGe:H layer thickness on the RTJ cells' performance was also investigated and summarized in Fig. S4. After fine-tuning the Ge content and the inner layer thickness, the RTJ cells can achieve a high V_{OC} of 1.2 V, J_{SC} of 11.0 mA/cm^2, *FF* of 61.5% and an overall conversion efficiency of $\eta = 8.1\%$, which largely outperform their single junction counterpart fabricated in the same batch, with typical V_{OC} of 0.8 V, J_{SC} of 12.4 mA/cm^2, *FF* of 58.6% and conversion efficiency of $\eta = 5.7\%$.

Compared to the co-deposited planar tandem a-Si:H/a-SiGe:H thin film cells (see the blue dashed line in Fig. 3b, with V_{OC} of 1.21 V, J_{SC} of 7.48 mA/cm^2), the V_{OC} of the RTJ cells is only slightly lower, indicating that the tandem *p-i-n* junctions deposited over the standing SiNWs by PECVD can preserve a high electric quality, without much degradation arising from possible coating inhomogeneities over such complex structures. Meanwhile, a much higher J_{SC} has been achieved by the RTJ cells, which highlight the critical role played by the beneficial light trapping realized within the 3D RTJ matrix. This contribution can be better revealed by comparing the external quantum efficiency (EQE) responses, in Fig. 4a and b which were measured under corresponding biased lights, of the outer/top a-Si:H and the inner/bottom a-SiGe:H junctions in 3D radial or planar architecture. It is shown that the EQE responses of both the a-Si:H and a-SiGe:H junctions in RTJ cells are significantly enhanced, particularly to the long wavelength ends, where the light absorption coefficients start to decrease and the contribution of light scattering among the 3D RTJ units becomes more prominent.

In order to gain further insights into the light absorption patterns or distributions within the 3D RTJ units, finite element simulation models of the RTJ cells were constructed by using the RF module of COMSOL analysis toolkit, like the simulation model built for the radial single junction cells in our previous works, except that a more complex RTJ structure is constructed with corresponding thin film materials. As detailed in Fig. S5, the optical properties (the *n-k* curves) of the thin film materials were extracted beforehand via the spectroscopic ellipsometry (SE) measurement and modeling of the same thin film materials deposited on planar substrate surface, which provide a solid basis to achieve a realistic simulation of the RTJ cells. For a standing RTJ unit, placed within a cubic box with periodic boundary conditions (as specified in Fig. S6) and under normal *y-axis* polarized incident, the calculated light absorption patterns extracted from the cross-section surfaces in the middle of the RTJ cells are presented in Fig. 4c for different incident wavelengths and with different Ge contents (labeled by GeH_4 flow rates) in the inner a-SiGe junction. It is found that, while the short wavelengths are mostly absorbed by the outer a-Si junction, the longer wavelengths $\lambda > 700$ nm can penetrate deeper into the RTJ multilayers and get absorbed by the inner a-SiGe:H layer. Apparently, a relatively high Ge content (flow rate > 20 SCCM) is necessary for an efficient light harnessing of the long wavelengths. Meanwhile, the calculated vertical light absorption patterns extracted from the *x-plane* and *y-plane* cross-sections, as well as the light absorption patterns for the planar cell

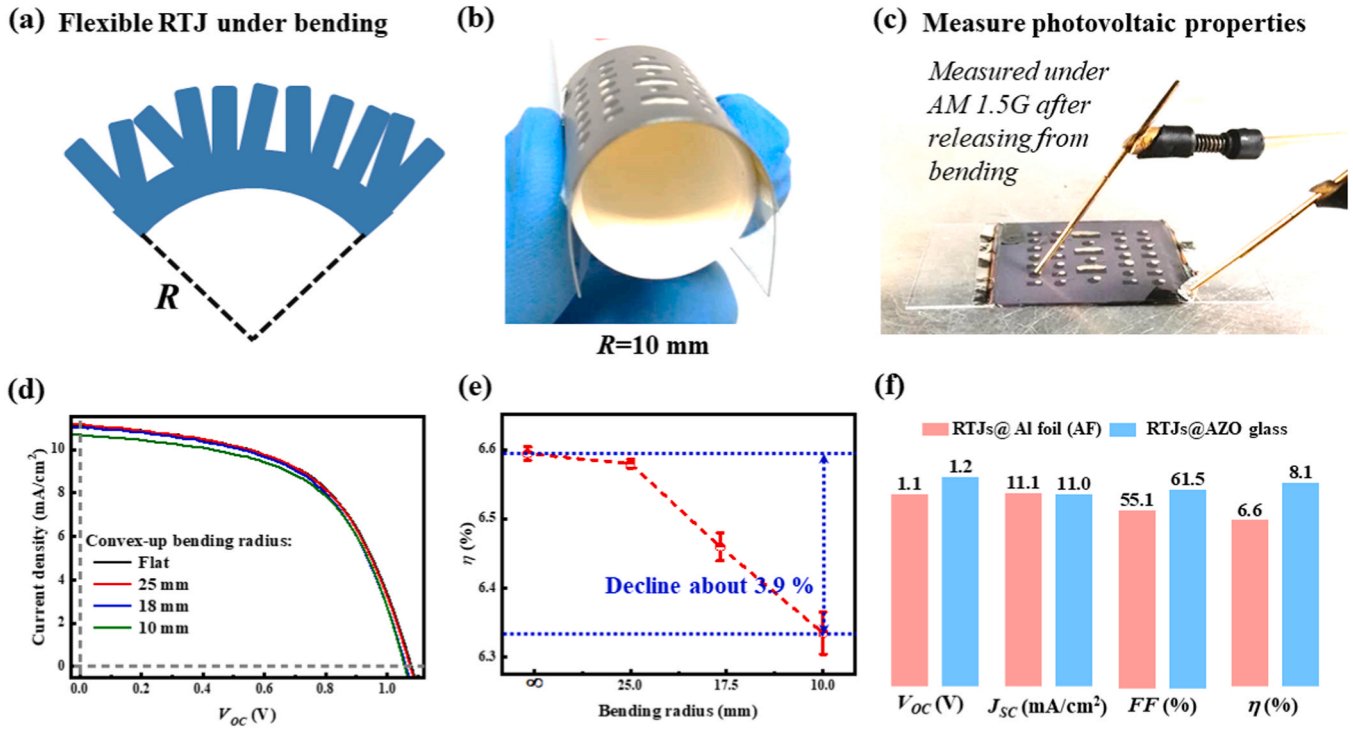

Fig. 5. (a) and (b) show the diagram and photograph of convex-up bending, respectively. The testing photograph after convex-up bending is presented in (c). The *J-V* curves vs different bending radius and the value of η vs different bending radius are shown in (d) and (e), respectively. The extracted performance parameters V_{OC}, J_{SC}, *FF* and η of RTJs fabricated on AZO glass and Al foil, are shown in (f), and compared in the histograms.

structures, are presented in Fig. S7. Obviously, the longer wavelength incidences ($\lambda > 700$ nm) can propagate deeper into the coaxial multi-layer RTJ cell units, while the short wavelength @400 nm is absorbed superficially. Compared to the calculated light absorption patterns in the planar structures, the RTJ solar cells achieve a stronger light absorption performance, especially for the long wavelengths, which can be attributed to the significant light trapping effect among the unique 3D RTJ framework.

Finally, the RTJ units can also be fabricated directly upon commercially-available aluminum foil (AF) with a thickness of only 15 μm, without any separation or protection layer between the RTJ and the Al substrate. The discrete SiNWs provide practical 3D supports that firmly stand/anchor on the relatively soft AF surface, while the photo-active RTJ portion coated on the standing SiNW cores are well separated/protected from detrimental strain or distortion accumulated on the AF surface, as depicted schematically in Fig. 5a. Compared to the RSJ units grown on flexible AF substrate demonstrated in our previous work [5], the RTJs@AF accomplish a much higher conversion efficiency η of 6.6%, which is ~20% higher than that of 5.6% for RSJs@AF. The solar cell performances of the flexible RTJs@AF cells to those built on solid AZO glass are also compared and summarized in Fig. 5f, where the V_{OC} and *FF* of 1.1 V and 55.1% are apparently lower than those of 1.2 V and 61.5% for the co-deposited RTJs@AZO glass. However, the RTJs@AF devices have a slightly higher J_{SC} of 11.1 mA/cm^2, over that of 11.0 mA/cm^2 for RTJs@AZO glass, which could arise from the beneficial bottom reflection effect provided by AF that increases the light harvesting for the RTJs upon AF substrate, while those on flat AZO glass substrate have no anti-reflection coating at the bottom. The flexibility of RTJs@AF cells was tested by attaching them to cylinder rods, as shown in Fig. 5b, with varied convex radii ranging from $R = 10$–25 mm. The evolution of the *J-V* curves measured under AM 1.5 G and after applying different bending conditions are presented in Fig. 5d. It is found that the conversion efficiency of the RTJs@AF solar cells experiences only a small 3.9% efficiency drop even after bending to 10 mm radius, as seen in Fig. 5e, accompanied with slightly decreased J_{SC} from 11.13 mA/cm^2 to 10.69 mA/cm^2 and V_{OC} from 1.08 V to 1.05 V. Moreover, the RTJs@AF demonstrate also an excellent flexibility and mechanical stability that can retain 87% PCE, 96% V_{OC} and 95% J_{SC} after 150 times convex-up bending to 10 mm radius, as shown in Fig. S8 measured for the samples fabricated in the same batch.

Remarkably, the RTJ thin film solar cells fabricated on AF substrates have achieved a new record of PTWR~1628 W/kg, nearly 700%, 400%, 500% and 20% improved compared to the flexible a-Si:H thin film solar cells in the literature [5,51–53], as summarized in Table 1. This figure-of-merit is particularly important for developing portable or wearable photovoltaic applications. It is also important to note this first experimental demonstration of 3D radial tandem solar cells over VLS-grown SiNWs can achieve simultaneously outstanding flexibility, good efficiency and high PTWR performance that have not been possible for the planar tandem solar cells.

In the future, this low temperature growth and fabrication strategy of RTJ solar cells could also be applied to other cheaper polymer and even cardboard (for example [54]) substrates to explore flexible thin film solar cells at extremely low cost. On the other hand, in order to boost the RTJ cell efficiency further, a wider bandgap window layer material can be used, such as μc-SiO_x:H that has higher transparency and much less absorption loss compared to the a-Si:H emitter used in this work, to improve both the V_{OC} and J_{SC} [55,56]. Or, the a-SiGe:H radial junction thin film cells can also combine with the wide bandgap perovskite thin film cells, as the top/outer junction, to achieve a hybrid tandem junction configuration similar to that described in Ref. [57]. Furthermore, more systematic parametric optimizations have to be carried out in the future, with the guidance of finite element modeling and simulation [58], to maximize the light harvesting performance in the complex 3D RTJ framework to yield even higher J_{SC}.

4. Conclusion

In summary, the first radial a-Si:H/a-SiGe:H tandem junction thin film solar cells have been successfully fabricated over VLS-grown SiNW matrices, with ultrathin absorber layers within the radially stacked *p-i-n* multilayers that allow for a broader spectral range absorption, higher photo-voltage output, and greatly improved device performance. An excellent flexibility and a record PTWR performance (~1628 W/kg) have been accomplished for the RTJ cells constructed directly upon thin AF substrates, which can bend down to 10 mm radius. These results highlight the benefits of implementing the advanced tandem solar cell design over 3D radial junction architecture to develop a new generation of Si-based high performance, flexible, light-weight and durable thin film photovoltaics.

CRediT authorship contribution statement

Shaobo Zhang: Conceptualization, Methodology, Formal analysis, Investigation, Data curation, Writing - original draft, Visualization, Software. **Ting Zhang:** Data curation. **Zongguang Liu:** Formal analysis, Data curation. **Junzhuan Wang:** Writing - review & editing, Resources, Software. **Linwei Yu:** Conceptualization, Methodology, Formal analysis, Investigation, Data curation, Writing - original draft, Writing - review & editing, Resources, Project administration, Funding acquisition, Supervision, Software. **Jun Xu:** Writing - review & editing, Resources. **Kunji Chen:** Writing - review & editing, Resources. **Pere Roca i Cabarrocas:** Formal analysis, Writing - review & editing.

Declaration of Competing Interest

The authors declare that they have no known competing financial interests or personal relationships that could have appeared to influence the work reported in this paper.

Table 1
Comparison of this work to other flexible a-Si:H thin film solar cells in the published literatures.

Substrate/Thickness (μm)	Absorber/Thickness (nm)	V_{OC} (V)	J_{SC} (mA/cm^2)	PCE (%)	Power-to-weight ratio (W/kg)	Reference
PI/No data	No data	~0.8	~1	3.2	200	[51]
Polyimide/20–30	400	6.5	1.6	5.8	340	[52]
Polyimide/20	400	14.0	0.5	4.4	275	[53]
Al foil/15	80	0.71	14.2	5.6	1382	[5]
Al foil/15	45/55	1.1	11.1	6.6	1628	This work

Acknowledgments

The authors acknowledge the financial support from the National Natural Science Foundation of China under Nos. 11874198, 61974064 and 61921005, National Key Research and Development Program of China (2018YFB2200101) and the Fundamental Research Funds for the Central Universities.

Appendix A. Supporting information

Supplementary data associated with this article can be found in the online version at doi:10.1016/j.nanoen.2021.106121.

References

[1] S. Kim, J.W. Chung, H. Lee, J. Park, Y. Heo, H.M. Lee, Remarkable progress in thin-film silicon solar cells using high-efficiency triple-junction technology, Sol. Energy Mater. Sol. Cells 119 (2013) 26–35.
[2] S. Okamoto, E. Maruyama, A. Terakawa, W. Shinohara, S. Nakano, Y. Hishikawa, K. Wakisaka, S. Kiyama, Towards large-area, high-efficiency a-Si/a-SiGe tandem solar cells, Sol. Energy Mater. Sol. Cells 66 (2001) 85–94.
[3] L. Yu, F. Fortuna, B. O'Donnell, T. Jeon, M. Foldyna, G. Picardi, P. Roca i Cabarrocas, Bismuth-catalyzed and doped silicon nanowires for one-pump-down fabrication of radial junction solar cells, Nano Lett. 12 (2012) 4153–4158.
[4] B. Liu, L. Bai, X. Zhang, C. Wei, Q. Huang, J. Sun, H. Ren, G. Hou, Y. Zhao, Fill factor improvement in PIN type hydrogenated amorphous silicon germanium thin film solar cells: omnipotent N type μc-SiO:H layer, Sol. Energy Mater. Sol. Cells 140 (2015) 450–456.
[5] X. Sun, T. Zhang, J. Wang, F. Yang, L. Xu, J. Xu, Y. Shi, K. Chen, P. Roca i Cabarrocas, L. Yu, Firmly standing three-dimensional radial junctions on soft aluminum foils enable extremely low cost flexible thin film solar cells with very high power-to-weight performance, Nano Energy 53 (2018) 83–90.
[6] H. Xiao, J. Wang, H. Huang, L. Lu, Q. Lin, Z. Fan, X. Chen, C. Jeong, X. Zhu, D. Li, Performance optimization of flexible a-Si:H solar cells with nanotextured plasmonic substrate by tuning the thickness of oxide spacer layer, Nano Energy 11 (2015) 78–87.
[7] R. Yang, C.H. Lee, B. Cui, A. Sazonov, Flexible semi-transparent a-Si:H pin solar cells for functional energy-harvesting applications, Mater. Sci. Eng.: B 229 (2018) 1–5.
[8] F. Yang, J. Wang, J. Lu, Z. Yu, L. Yu, J. Xu, Y. Shi, K. Chen, P. Roca i Cabarrocas, Biomimetic radial tandem junction photodetector with natural RGB color discrimination capability, Adv. Opt. Mater. 5 (2017), 1700390.
[9] Z. Liu, B. Wen, L. Cao, S. Zhang, Y. Lei, G. Zhao, L. Chen, J. Wang, Y. Shi, J. Xu, X. Pan, L. Yu, Photoelectric cardiac pacing by flexible and degradable amorphous Si radial junction stimulators, Adv. Healthc. Mater. 9 (2019), 1901342.
[10] F. Meillaud, A. Shah, C. Droz, E. Vallat-Sauvain, C. Miazza, Efficiency limits for single-junction and tandem solar cells, Sol. Energy Mater. Sol. Cells 90 (2006) 2952–2959.
[11] H. Keppner, J. Meier, P. Torres, D. Fischer, A. Shah, Microcrystalline silicon and micromorph tandem solar cells, Appl. Phys. A Mater. Sci. Process. 69 (1999) 169–177.
[12] C.Y. Tsai, C.Y. Tsai, Tandem amorphous/microcrystalline silicon thin-film solar modules: developments of novel technologies, Sol. Energy 170 (2018) 419–429.
[13] T. Söderström, F.J. Haug, X. Niquille, V. Terrazzoni, C. Ballif, Asymmetric intermediate reflector for tandem micromorph thin film silicon solar cells, Appl. Phys. Lett. 94 (2009), 063501.
[14] J. Jung, S. Kim, C. Shin, J. Park, J. Yi, Backside etching process for enhancing the light trapping capacity and electrical properties of micromorph tandem solar cells, J. Nanosci. Nanotechnol. 17 (2017) 8158–8162.
[15] L. Bai, B. Liu, J. Fan, D. Zhang, C. Wei, J. Sun, Y. Zhao, X. Zhang, J. Power Sources 266 (2014) 138–144.
[16] S.W. Liang, Y.T. Huang, H.J. Hsu, C.H. Hsu, C.C. Tsai, Applications of μc-SiOx:H as integrated n-layer and back transparent conductive oxide for a-Si:H/μc-Si:H tandem cells, Jpn. J. Appl. Phys. 53 (2014) 05FV08.
[17] A. Terakawa, Review of thin-film silicon deposition techniques for high-efficiency solar cells developed at Panasonic/Sanyo, Sol. Energy Mater. Sol. Cells 119 (2013) 204–208.
[18] M. Gharghi, E. Fathi, B. Kante, S. Sivoththaman, X. Zhang, Heterojunction silicon microwire solar cells, Nano Lett. 12 (2012) 6278–6282.
[19] Z. Fan, R. Kapadia, P.W. Leu, X. Zhang, Y.-L. Chueh, K. Takei, K. Yu, A. Jamshidi, A.A. Rathore, D.J. Ruebusch, M. Wu, A. Javey, Ordered arrays of dual-diameter nanopillars for maximized optical absorption, Nano Lett. 10 (2010) 3823–3827.
[20] K.Q. Peng, S.T. Lee, Silicon nanowires for photovoltaic solar energy conversion, Adv. Mater. 23 (2011) 198–215.
[21] V. Sivakov, G. Andrä, A. Gawlik, A. Berger, J. Plentz, F. Falk, S.H. Christiansen, Silicon nanowire-based solar cells on glass: synthesis, optical properties, and cell parameters, Nano Lett. 9 (2009) 1549–1554.
[22] X. Wang, K.L. Pey, C.H. Yip, E.A. Fitzgerald, D.A. Antoniadis, Vertically arrayed Si nanowire/nanorod-based core-shell p-n junction solar cells, J. Appl. Phys. 108 (2010), 124303.
[23] M.D. Kelzenberg, S. Boettcher, J.A. Petykiewicz, D.B. Turner-Evans, M.C. Putnam, E.L. Warren, J.M. Spurgeon, R.M. Briggs, N.S. Lewis, H.A. Atwater, Enhanced absorption and carrier collection in Si wire arrays for photovoltaic applications, Nat. Mater. 9 (2010) 239–244.
[24] S. Zhang, T. Zhang, L. Cao, Z. Liu, J. Wang, J. Xu, K. Chen, L. Yu, Coupled boron-doping and geometry control of tin-catalyzed silicon nanowires for high performance radial junction photovoltaics, Opt. Express 27 (2019) 37248–37256.
[25] Z. Yu, J. Lu, S. Qian, S. Misra, L. Yu, J. Xu, L. Xu, J. Wang, Y. Shi, K. Chen, P. Roca i Cabarrocas, Bi-Sn alloy catalyst for simultaneous morphology and doping control of silicon nanowires in radial junction solar cells, Appl. Phys. Lett. 107 (2015), 163105.
[26] S. Misra, L. Yu, M. Foldyna, P. Roca i Cabarrocas, Readability analysis of healthcare-oriented education resources from the American Academy of Facial Plastic and Reconstructive Surgery, Laryngoscope 123 (2013), 90-6.
[27] S. Misra, L. Yu, W. Chen, M. Foldyna, P. Roca i Cabarrocas, A review on plasma-assisted VLS synthesis of silicon nanowires and radial junction solar cells, J. Phys. D Appl. Phys. 47 (2014), 393001.
[28] L. Yu, S. Misra, J. Wang, S. Qian, M. Foldyna, J. Xu, Y. Shi, E. Johnson, P. Roca i Cabarrocas, Understanding light harvesting in radial junction amorphous silicon thin film solar cells, Sci. Rep. 4 (2014) 4357.
[29] J. Cho, B. O'Donnell, L. Yu, K.-H. Kim, I. Ngo, P. Roca i Cabarrocas, Prog. Photovolt. Res. Appl. 21 (2013) 77–81.
[30] P. Roca i Cabarrocas, Plasma enhanced chemical vapor deposition of amorphous, polymorphous and microcrystalline silicon films, J. Noncryst. Solids 266–269 (2000) 31–37.
[31] B. Kalache, A.I. Kosarev, R. Vanderhaghen, P. Roca i Cabarrocas, Ion bombardment effects on the microcrystalline silicon growth mechanisms and structure, J. Noncryst. Solids 299–302 (2002) 63–67.
[32] L.W. Veldhuizen, R.E.I.S.Y. Kuang, Ultrathin tandem solar cells on nanorod morphology with 35-nm thick hydrogenated amorphous silicon germanium bottom cell absorber layer, Sol. Energy Mater. Sol. Cells 158 (2016) 209–213.
[33] D.W. Kang, S.W. Ahn, H.M. Lee, M.K. Han, Effect of TiO_2 antireflection layer with various conductivities and refractive indices on performance of amorphous silicon/amorphous silicon germanium tandem solar cells, Jpn. J. Appl. Phys. 51 (2012) 10NB10.
[34] E. Maruyama, S. Okamoto, A. Terakawa, W. Shinohara, M. Tanaka, S. Kiyama, Toward stabilized 10% efficiency of large-area (>5000cm2) a-Si/a-SiGe tandem solar cells using high-rate deposition, Sol. Energy Mater. Sol. Cells 74 (2002) 339–349.
[35] Q.H. Fan, C. Chen, X. Liao, X. Xiang, S. Zhang, W. Ingler, N. Adiga, Z. Hu, X. Cao, W. Du, X. Deng, High efficiency silicon–germanium thin film solar cells using graded absorber layer, Sol. Energy Mater. Sol. Cells 94 (2010) 1300–1302.
[36] S. Guha, J. Yang, A. Pawlikiewicz, T. Glatfelter, R. Ross, S.R. Ovshinsky, Band-gap profiling for improving the efficiency of amorphous silicon alloy solar cells, Appl. Phys. Lett. 54 (1989) 2330–2332.
[37] J. Yang, A. Banerjee, S. Guha, Triple-junction amorphous silicon alloy solar cell with 14.6% initial and 13.0% stable conversion efficiencies, Appl. Phys. Lett. 70 (1997) 2975–2977.
[38] J.W. Schüttauf, B. Niesen, L. Löfgren, M. Bonnet Eymard, M. Stuckelberger, S. Hänni, M. Boccard, G. Bugnon, M. Despeisse, F.J. Haug, F. Meillaud, C. Ballif, Amorphous silicon–germanium for triple and quadruple junction thin-film silicon based solar cells, Sol. Energy Mater. Sol. Cells 133 (2015) 163–169.
[39] S. Misra, Thesis, 2015. http://www.theses.fr/2015EPXX0062.
[40] H. Xu, L. Yin, C. Liu, X. Sheng, N. Zhao, Recent advances in biointegrated optoelectronic devices, Adv. Mater. 30 (2018), 1800156.
[41] Z. Lou, L. Li, L. Wang, G. Shen, Recent progress of self-powered sensing systems for wearable electronics, Small 13 (2017), 1701791.
[42] S.A. Hashemi, S. Ramakrishna, A.G. Aberle, Recent progress in flexible–wearable solar cells for self-powered electronic devices, Energy Environ. Sci. 13 (2020) 685–743.
[43] P.K. Chang, C.H. Lu, C.H. Yeh, M.P. Houng, High efficiency a-Si:H/a-Si:H solar cell with a tunnel recombination junction and a n-type μc-Si:H layer, Thin Solid Films 520 (2012) 3684–3687.
[44] S. Inthisang, T. Krajangsang, A. Hongsingthong, A. Limmanee, S. Kittisontirak, S. Jaroensathainchok, A. Moolakorn, A. Dousse, J. Sritharathikhun, K. Sriprapha, High efficiency a-Si:H/a-SiGe:H tandem solar cells fabricated with the combination of V- and U-shaped band gap profiling techniques, Jpn. J. Appl. Phys. 54 (2015), 08KB08.
[45] G. Hou, Q. Fan, X. Liao, C. Chen, X. Xiang, X. Deng, High-efficiency and highly stable a-Si:H solar cells deposited at high rate (8 Å/s) with disilane grading process, J. Vac. Sci. Technol. A Vac. Surf. Films 29 (2011), 061201.
[46] S. Gupta, G. Morell, B.R. Weiner, Role of H in hot-wire deposited a-Si:H films revisited: optical characterization and modeling, J. Non-Cryst. Solids 343 (2004) 131–142.
[47] S. Gupta, B.R. Weiner, G. Morell, Interplay of hydrogen and deposition temperature in optical properties of hot-wire deposited a-Si:H Films:Ex situspectroscopic ellipsometry studies, J. Vac. Sci. Technol. A Vac. Surf. Films 23 (2005) 1668–1675.
[48] G. Nakamura, K. Sato, Y. Yukimoto, K. Shirahata, T. Murahashi, K. Fujiwara, Amorphous SiGe: H for high performance solar cells, Jpn. J. Appl. Phys. 20 (1981) 291–296.
[49] S.S. Hegedus, E.A. Fagen, Midgap states ina-Si:H anda-SiGe:Hp-i-nsolar cells and Schottky junctions by capacitance techniques, J. Appl. Phys. 71 (1992) 5941–5951.
[50] L.W. Veldhuizen, C.H.M. van der Werf, Y. Kuang, N.J. Bakker, S.J. Yun, R.E. I. Schropp, Optimization of hydrogenated amorphous silicon germanium thin films and solar cells deposited by hot wire chemical vapor deposition, Thin Solid Films 595 (2015) 226–230.

[51] H. Cai, D. Zhang, Y. Xue, K. Tao, Study on diffusion barrier layer of silicon-based thin-film solar cells on polyimide substrate, Sol. Energy Mater. Sol. Cells 93 (2009) 1959–1962.
[52] H. Nishiwaki, K. Uchihashi, K. Takaoka, M. Nakagawa, H. Inoue, A. Takeoka, S. Tsuda, M. Ohnishi, Development of an ultralight, flexible a-Si solar cell submodule, Sol. Energy Mater. Sol. Cells 37 (1995) 295–306.
[53] Y. Kishi, H. Inoue, K. Murata, S. Kouzuma, M. Morizane, H. Shibuya, H. Nishiwaki, Y. Kuwano, A New Type of ultralight flexible a-Si Solar Cell, Jpn. J. Appl. Phys. 31 (1992) 12–17.
[54] A. Pimentel, A. Araújo, B. Coelho, D. Nunes, M. Oliveira, M. Mendes, H. Águas, R. Martins, E. Fortunato, 3D ZnO/Ag surface-enhanced raman scattering on disposable and flexible cardboard platforms, Materials 10 (2017) 1351.
[55] S. Misra, L. Yu, M. Foldyna, P. Roca i Cabarrocas, New approaches to improve the performance of thin-film radial junction solar cells built over silicon nanowire arrays, IEEE J. Photovolt. 5 (2015) 40–45.
[56] S. Qian, S. Misra, J. Lu, Z. Yu, L. Yu, J. Xu, J. Wang, L. Xu, Y. Shi, K. Chen, P. Roca i Cabarrocas, Full potential of radial junction Si thin film solar cells with advanced junction materials and design, Appl. Phys. Lett. 107 (2015), 043902.
[57] M. Chapa, M.F. Alexandre, M.J. Mendes, H. Águas, E. Fortunato, R. Martins, All-thin-film perovskite/C–Si four-terminal tandems: interlayer and intermediate contacts optimization, ACS Appl. Energy Mater. 2 (2019) 3979–3985.
[58] M.J. Mendes, S. Haque, O. Sanchez-Sobrado, A. Araujo, H. Aguas, E. Fortunato, R. Martins, Optimal-enhanced solar cell ultra-thinning with broadband nanophotonic light capture, iScience 3 (2018) 238–254.

Shaobo Zhang received the Bachelor degree and Master degree from China University of Mining and Technology in 2015 and 2018, respectively. He is currently a PhD candidate in the School of Electronic Science and Engineering, Nanjing University. His research interests include a-Si:H based radial junction thin film solar cells and photodetectors.

Ting Zhang graduated from Hefei University of Technology as a master and is now a PhD candidate in school of electronic science and engineering, Nanjing University. His research interests include semiconductor nanowire preparation and flexible nanowire electronics.

Zongguang Liu received his master degree from Southwest Jiaotong University in 2014 and his PhD degree in materials from Zhejiang University in 2018. He then was a Postdoctoral Researcher at School of electronic science and engineering, Nanjing University. He is currently an Associated Researcher in Nanjing University. His research interests include the silicon nanowire-based biosensors, flexible electronics and photovoltaic devices.

Junzhuan Wang is an Associate Professor in School of Electronic Science and Engineering, Nanjing University, China. She got her PhD in Applied Physics, Nanjing University in 2008 and joined the National Laboratory of Solid State Microstructures, Nanjing University. From 2009 to 2011 she was in LPICM, Ecole Polytechnique/CNRS as a visiting scholar. Dr. Wang's research focuses on the semiconductor nanomaterials for photonic devices and spectrum sensors. She has published around 50 peer reviewed papers, including in Nature Communications, Advanced Materials, Nano Letters and Advanced Optical Materials.

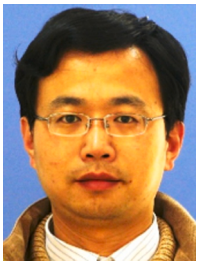

Linwei Yu received the BS degree in semiconductor physics in 2001 and the PhD degree in microelectronics from Nanjing University, Nanjing, China, in 2007. From 2007 to 2009, he was a Postdoctoral Researcher in LPICM, Ecole Polytechnique, France, and then joined CNRS as a Permanent Researcher (CR2) in 2009. Since 2013, he has been a Professor with the School of Electronics Science and Engineering, Nanjing University. His research interests include the growth mechanism and application of silicon nanowires for stretchable thin film electronics, 3D logics, sensors and photovoltaics.

Jun Xu received the BS degree in physics and the PhD degree in microelectronics both from Nanjing University, Nanjing, China, in 1989 and 1995, respectively. In 1996, he was a member of the National Laboratory of Solid State Microstructures, Nanjing University. Since 2004, he has been a Professor in the Department of Physics and School of Electronic Science and Engineering. He worked as a Visiting Researcher in the Department of Electronic Engineering, Hongkong Chinese University, in 2000 and the Graduate School of Advanced Science of Matter, Hiroshima University, Japan, in 2005. His research interests include silicon-based amorphous materials, semiconductor nanostructures, and optoelectronic devices.

Kunji Chen received the Graduate degree from Nanjing University, Nanjing, China, in 1963. From 1981 to 1983, he was a Visiting Scholar studying at the University of Chicago, Chicago, IL, USA. Since then he had eight times to go to the Universities and Institutes of United State and Japan for cooperation research work. He is currently a Professor at Nanjing University. His research interests include nanosemiconductor materials, quantum nanoelectronics, and nanooptoelectronics. Prof. Chen has received many awards including the National Nature Science Award in 2003 and the Advanced Achievements Award in Science and Technology of Jiangsu Province (1988, 1995, and 2002). In 1996, he was elected as a member of the International Advisory Committee of International Conference on Amorphous and Nanocrystalline Semiconductors (ICANS).

Pere Roca i Cabarrocas obtained his PhD from University Paris VII in 1988. After a post-doc at Princeton he joined LPICM laboratory at Ecole Polytechnique, that he directed from 2012 to 2020. He is currently scientific director of IPVF. During his career he has developed plasma deposition processes for silicon based thin films, nanocrystals, epitaxial layers, and nanowires; as well as their application to solar cells and thin film transistors. He received the Ecole Polytechnique Innovation Award 2009 and the CNRS Silver medal in 2011. He has over 500 papers, holds 38 patents and has supervised 50 PhD students.